

# A New Method for Localizing the Sources of Correlated Cross-Frequency Oscillations in Human Brains

Hiroaki Tanaka, Yuki Hayashida, Tomohiko Igasaki, Nobuki Murayama

**Abstract**—Anatomically distributed areas are dynamically linked to form functional networks for processing and integrating the different modalities of information in the human brain. A part of such networks is considered to be realized with synchronization of neuronal activities, which can generate correlated neural oscillation at the same and/or different frequency bands. To investigate the networks with the synchronization, analysis of connectivity between not only same frequency oscillation but also different frequency (i.e. cross-frequency) is needed. For source estimation with electroencephalogram (EEG) or magneto-encephalogram (MEG) signals, a spatial filtering technique is recently applied as an alternative method for equivalent current dipole (ECD) estimation technique. Non-adaptive type of spatial filtering technique, such as the Standardized low-resolution brain electromagnetic tomography (sLORETA), is reported to discriminate correlated sources. However, it may lead to inaccurate results due to its low spatial resolution. In the present study, we proposed a new systematic approach for localizing the sources of correlated cross-frequency oscillations. The method we propose can overcome the limitation of the non-adaptive spatial filtering technique by proactively using identified information in sensor level analysis (e.g. cross-correlation map and correlation topography), which allow us to focus on target sources. The performance of our proposed method is evaluated with simulated EEG signals, and is compared with traditional method.

## I. INTRODUCTION

FOR processing and integrating the different modalities of information in the human brain, anatomically distributed areas are dynamically linked to form functional networks. A part of such networks is considered to be realized with the synchronization of neuronal activities, which can generate correlated neural oscillations at the same and/or different frequency bands, as found in previous studies: e.g. correlated activities between alpha and gamma bands during perception and memory tasks [1], alpha/beta and gamma

bands during motor imagery tasks [2].

Although one would be aware of the ill-posed inverse problem in estimating the source location of neural oscillations from the electro-encephalogram (EEG) or magneto-encephalogram (MEG), many methods for such estimation have been proposed, and applied to the experimental data, in previous studies. Here, we propose a new systematic approach for localizing the sources of correlated cross-frequency oscillations from the EEG signals. And the performance of our method is evaluated with using simulated EEG signals, and is compared with that of a traditional method.

## II. MATERIAL AND METHOD

### A. Technical Method

The method we propose is based on the temporal correlation between a pair of the magnitude of a Fourier spectrum obtained for the two signals; and on extraction of a pair of the spectral signals that exhibit significant correlation with each other, to subsequently localize the signal sources.

#### 1) Definitions

Recorded data of a reference EEG signal (or possibly, a signal of electromyography (EMG) or MEG) and of a test signal from the other EEG sensors are denoted as  $b_{ref}(t)$  and  $b_i(t)$ , respectively (where  $i = 1 \dots N_c$ ;  $N_c$  is channel count of sensors). Each of these data are divided into sections by applying a sliding time window with overlap and Fourier spectra are computed for every section. Each of the sections is represented as  $b_{ref}^j(t)$  or  $b_i^k(t)$  (where  $j, k = 1 \dots N_e$ ;  $N_e$  is the number of sections). The magnitude of a Fourier spectrum in each section is denoted as  $\mathbf{B}_{ref}^j(f_{ref-l})$ , or  $\mathbf{B}_i^k(f_m)$  (where  $l, m = 1 \dots N_f$ ;  $N_f$  is the number of spectrum). The Spearman's rank correlation coefficient between these spectrum magnitude,  $\gamma_i(f_{ref-l}, f_m)$  is calculated by

$$\gamma_i(f_{ref-l}, f_m) = \frac{\sum_{j=1}^{N_e} (r(\mathbf{B}_{ref}^j(f_{ref-l})) - \overline{r(\mathbf{B}_{ref}^j(f_{ref-l}))}) (r(\mathbf{B}_i^j(f_m)) - \overline{r(\mathbf{B}_i^j(f_m))}))}{\sqrt{\sum_{j=1}^{N_e} (r(\mathbf{B}_{ref}^j(f_{ref-l})) - \overline{r(\mathbf{B}_{ref}^j(f_{ref-l}))})^2} \sqrt{\sum_{k=1}^{N_e} (r(\mathbf{B}_i^k(f_m)) - \overline{r(\mathbf{B}_i^k(f_m))})^2}}$$

where  $r(\cdot)$  denotes the rank and  $\overline{r(\mathbf{B}_{ref}^j(f_{ref-l}))}$ ,  $\overline{r(\mathbf{B}_i^j(f_m))}$  are averages of the rank, namely;

Hiroaki Tanaka is with Graduate School of Science and Technology, Kumamoto University; 2-39-1 Kurokami, Kumamoto-shi, Kumamoto 860-8555, Japan (e-mail: 097d9307@st.kumamoto-u.ac.jp).

Yuki Hayashida was with Graduate School of Science and Technology, Kumamoto University; 2-39-1 Kurokami, Kumamoto-shi, Kumamoto 860-8555, Japan. He is currently with Graduate School of Engineering, Osaka University; 2-1 Yamadaoka, Suita-shi, Osaka 565-0871, Japan (e-mail: hayashida@eei.eng.osaka-u.ac.jp).

Tomohiko Igasaki is with Graduate School of Science and Technology, Kumamoto University; 2-39-1 Kurokami, Kumamoto-shi, Kumamoto 860-8555, Japan (e-mail: iga@cs.kumamoto-u.ac.jp).

Nobuki Murayama is with Graduate School of Science and Technology, Kumamoto University; 2-39-1 Kurokami, Kumamoto-shi, Kumamoto 860-8555, Japan. (e-mail: murayama@cs.kumamoto-u.ac.jp).

$$\overline{r(\mathbf{B}_{ref}(f_{ref-l}))} = \frac{1}{Ne} \sum_{j=1}^{Ne} r(|\mathbf{B}_{ref}^j(f_{ref-l})|), \quad \overline{r(\mathbf{B}_i(f_m))} = \frac{1}{Ne} \sum_{k=1}^{Ne} r(|\mathbf{B}_i^k(f_m)|)$$

## 2) Sensor level analysis

The sets of the correlation coefficient (i.e.  $\gamma_i(f_l, f_m)$   $|i = 1 \dots N_c; l, m = 1 \dots N_f$ ) can be visualized in the cross-spectral plots with respect to certain combinations of reference and test signals/sensors (as in Fig. 2A), or in the topographical maps with respect to certain combinations of frequencies (as in Fig. 2B, C). These visualizations enable one to select a frequency pair  $(f_{ref-l}, f_m)$  showing significant positive or negative correlation, and subsequently, to map topographically the correlation coefficient vector  $\boldsymbol{\gamma} = [\gamma_1, \gamma_2, \dots, \gamma_{N_c}]^T$  at this frequency pair.

## 3) Source estimation

In this step, source estimation is performed based on the sensor level analysis described above. The correlation topography is used for weighting the sensor signals to target the activities that show significant correlation with each other.

For source estimation, spatial filtering technique is recently used as an alternative method for equivalent current dipole (ECD) estimation technique, however it has limitations. For instance, adaptive type of spatial filtering technique can not discriminate correlated sources, while non-adaptive type can not distinguish proximal sources due to its lower spatial resolution [3]. While considering the limitation of spatial filtering technique, we employ non-adaptive spatial filtering technique to achieve our purpose to localize correlated sources.

A spatial filtering technique is generally defined as linear combination of time constant weight vector and recorded data described as

$$\hat{\mathbf{s}}_i(t) = \mathbf{w}_i^T \mathbf{b}(t)$$

where  $\hat{\mathbf{s}}_i(t)$  is estimated source in time domain at i-th voxel set in the brain area,  $\mathbf{w}_i = [w_i^1, w_i^2, \dots, w_i^{N_c}]^T$ ;  $w_i^k$  is weight from k-th sensor to source at i-th voxel in the brain, and  $\mathbf{b}(t) = [b_1(t), b_2(t), \dots, b_{N_c}(t)]^T$  indicate a column vector of recorded data [4]. Because this formula is linear operation, spatial filtering calculation can be performed in frequency domain, namely;

$$\hat{\mathbf{S}}_i(f) = FT(\mathbf{w}_i^T \mathbf{b}(t)) = \mathbf{w}_i^T FT(\mathbf{b}(t)) = \mathbf{w}_i^T \mathbf{B}(f)$$

where  $FT(\cdot)$  denotes Fourier transform (FT) operation and  $\mathbf{B}(f) = [\mathbf{B}_1(f), \mathbf{B}_2(f), \dots, \mathbf{B}_{N_c}(f)]^T$ ,  $\mathbf{B}_i(f) = FT(b_i(t))$ ,  $i = 1 \dots N_c$ . Consequently, frequency characteristic of sources can be directly estimated from FT of sensor signals. This means that if target frequency can be identified previously (i.e. sensor level analysis), higher signal to noise estimation can be achieved, because non-target activities in other frequency

bands can be excluded.

And to focus on target correlated sources, FT of recorded data are weighted by using vector  $(\mathbf{w}_c = [w_{c_1}, w_{c_2}, \dots, w_{c_{N_c}}]^T)$ , which is derived from the correlation coefficient vector, as below,

$$\mathbf{B}_w^k(f) = \text{diag}(\mathbf{w}_c) \mathbf{B}^k(f) = \begin{bmatrix} w_{c_1} & 0 & 0 & 0 \\ 0 & w_{c_2} & 0 & 0 \\ 0 & 0 & \ddots & 0 \\ 0 & 0 & 0 & w_{c_{N_c}} \end{bmatrix} \mathbf{B}^k(f)$$

$$= [w_{c_1} \mathbf{B}_1^k(f), w_{c_2} \mathbf{B}_2^k(f), \dots, w_{c_{N_c}} \mathbf{B}_{N_c}^k(f)]^T$$

where  $\mathbf{B}_w^k(f)$  is weighted FT of recorded data of section  $k = 1 \dots Ne$  and  $\mathbf{B}^k(f)$  is FT of recorded data.

Then, for source estimation, we employ the Standardized low-resolution brain electromagnetic tomography (sLORETA) as non-adaptive spatial filtering technique which was reported previously [5] and has no localization bias under ideal conditions [3]. Although the sLORETA weighted by correlation topography is considered to estimate significant correlated sources, the estimated sources averaged among all sections may become blurred due to wide skirts caused by lower spatial resolution of the sLORETA. Therefore, in order to avoid the blurred results and to achieve higher detection ability of correlated sources, we combine source quantification using the sLORETA-qm [6] and modulating of each section's spectra magnitude by reference at  $f_{ref-l}$  (i.e.  $\mathbf{B}_{ref}^j(f_{ref-l})$ ;  $j = 1 \dots N_e$ ) before averaging among all sections. The sLORETA-qm is a modified sLORETA for quantitative analysis which also have been applied to clinical application by evaluating spontaneous neuronal brain activity [7]. The combination effectively allow us to detect correlated sources because non-correlated sources are suppressed by the quantification through all sections. This procedure is described as below.

$$\begin{aligned} \hat{\mathbf{S}}_i^k(f_m) &\Rightarrow \text{weighting} : \mathbf{B}_{ref}^j(f_{ref-l}) \cdot \hat{\mathbf{S}}_i^k(f_m) \\ &\Rightarrow \text{quantification} : \hat{\mathbf{S}}_{i-q}^k(f_m) \\ &\Rightarrow \text{averaging} : \sum_{k=1}^{N_e} \hat{\mathbf{S}}_{i-q}^k(f_m) \end{aligned}$$

where  $\hat{\mathbf{S}}_{i-q}^k(f_m)$  is quantified estimated source by sLORETA-qm.

## B. Evaluation with simulated motor imagery task data

To assess accuracy of source localization by this approach, we evaluated it with simulated data.

The simulated data were supposed as motor imagery task [2], which had beta activity in motor area and negative correlated gamma activity in parieto-occipital area.

TABLE I  
CHARACTERISTICS OF SIMULATED SOURCES

Source No.	Location (MRI coordinate [mm])	Direction	Peak intensity [nAm]	Frequency [Hz]	Rising time [ms]	Peak time [ms]
S1	Left motor area (36.4, 9.9, 57.2)	Anterior to Posterior	Sustain: 80 Depth: 40 to 80	20	450 to 500	1000
S2	Left parieto-occipital area (26.4, 40.0, 27.2)	Posterior to Anterior	10	50	270 to 300	900 to 1000
S3	Left occipital area (6.4, 49.9, 7.2)	Anterior to Posterior		50	Continuous sin wave	

### 1) Sources location and waveform

Three equivalent current dipoles were simulated and located referring magnetic resonance image (MRI) of normal subject (37 y.o., male) as s1: beta activity (20[Hz]) on left motor area, s2: gamma activity (50[Hz]) on left parieto-occipital area and s3: spontaneous activity on left occipital area with same frequency as s2 (50[Hz]). The third source (s3) replicated alpha activity, however its frequency is set to 50[Hz] same as the second source (s2) so as to show whether our proposed method can extract only correlated source or not even in same frequency. The characteristics of those sources were summarized in Table 1, and waveforms were shown in Fig. 1. Depth of intensity of s1, peak intensity of s2, rising time of s1 and s2, and peak time of s2 were fluctuated. One epoch data included transiently reduced beta activity, gamma activity synchronized with the reduction of beta activity, and continuous alpha activity (50[Hz]) in time period of 2.5 [s] and with sampling rate of 500 [Hz]. Totally 100 epochs data were combined and used for analysis.

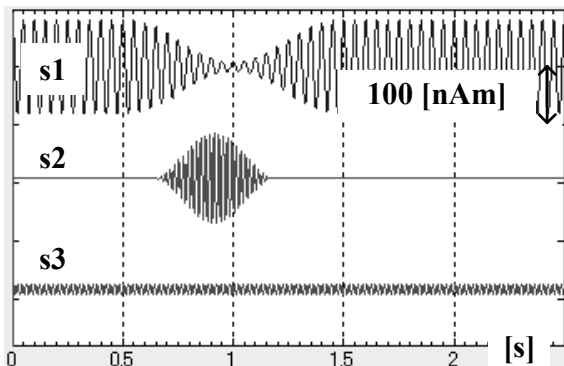


Fig. 1. Simulated waveform of each source in one epoch.

### 2) Forward modeling and sensor signals

Each EEG sensor was located corresponding with international 10-20 system by referring the MRI. Sensor signals were calculated with 4 layers spherical head model [8] fit to the MRI, and added white noise of 16 signal-to-ratio. sLORETA(-qm) was performed with 10mm of voxel spacing in the brain.

## III. RESULTS

### A. Sensor level analysis

Cross-frequency correlation was calculated under the

condition of 2[s] time window, 50% overlap and Hanning window function (time section count was 249).

At the first, we selected C3 as reference signal because significant activity was observed on the left side and C3 was centered among electrodes on the left side. Then, cross-frequency map of Cz with respect to C3 as reference signal because this map clearly showed frequency pair between around 50[Hz] of Cz and 20[Hz], 50[Hz] of C3 comparing with other maps. In the cross-frequency map, significant negative correlation (-0.87;  $p < 0.001$ ) was observed at frequency pair of (C3: 20[Hz], Cz: 51[Hz]) as shown in Fig. 2-(A) and corresponding correlation topography was shown in Fig. 2-(B). From this result, we next derived correlation topography of EEG signals of 20[Hz] with respect to Cz of 51[Hz] as shown in Fig. 2-(C). These correlation topographies were used as sensor signal weight for further source estimation.

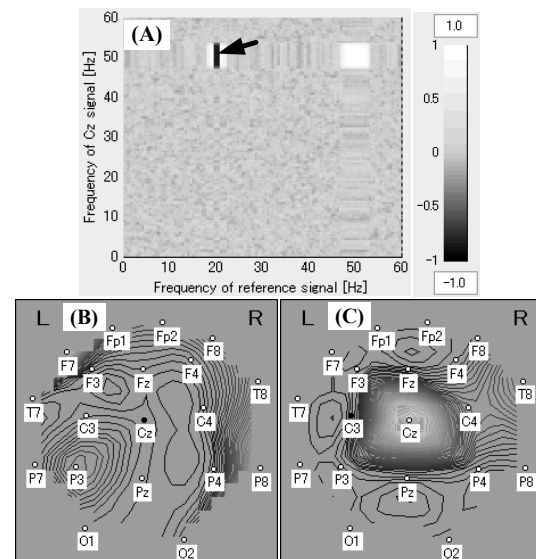


Fig. 2. Results of sensor level analysis: (A) Cross-frequency correlation map between signal of C3 as reference signal and signal of Cz, calculated under the condition of 2[s] time window, 50% overlap and Hanning window function. (B) Correlation topography of EEG signals of 51 [Hz] with respect to 20 [Hz] of C3 as reference signal (corresponding to black arrow indicated in (A)). (C) Correlation topography of EEG signals of 20 [Hz] with respect to 51 [Hz] of Cz as reference signal

### B. Source level analysis

In accordance with proposed approach, source estimation in frequency domain was performed at frequency of (20, 51 [Hz]) and with sensor signal weighting by the correlation

topographies which identified in sensor level analysis. Estimated sources are observed as voxels whose intensity is spatially max or local max voxel [6].

For frequency of 20 [Hz], we obtained only one source whose location was [36.4, 9.9, 57.2][mm], which completely corresponded with the simulated location of s1 (Fig. 3-(A)). For frequency of 50 [Hz], we obtained three sources. Maximum intensity source located on [26.4, 40.0, 27.2][mm], which completely coincided with the simulated location of s2, while intensities of remaining sources were lower than 5% of the maximum intensity (Fig. 3-(B)). And source level correlation between the sources of 20[Hz] and 50[Hz] was validated as -0.66. Note that the third source (s3) was not estimated even though it also has frequency of 50[Hz]. This means that our proposed method can estimate only correlated sources.

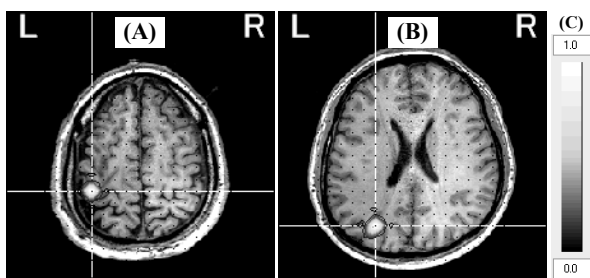


Fig. 3. Estimated sources superimposed on MR image.: (A) Source of 20 [Hz] correlated with 50 [Hz] signal of Cz. (B) Source of 50 [Hz] correlated with 20 [Hz] signal of C3. (C) Gray scale color bar indicating corresponding intensity.

### C. Source estimation by conventional method

To show advantage of the proposed method, we also calculated with conventional method, that is, frequency domain sLORETA/sLORETA-qm without information from sensor level analysis except frequency pair of 20 and 50 [Hz].

One source of 20 [Hz] was observed and it located on [36.4 9.9 57.2][mm] completely corresponded with one of s2. For frequency of 50[Hz], two estimated sources were detected. The first source with maximum intensity normalized as 1.0 located on [26.4, 40.0, 27.2][mm] completely corresponded to location of s2. The second source with intensity of 0.80 located on [6.4, 50.0, 7.2] [mm] which is completely same as location of s3. Source level correlation between source of 20[Hz] (s1) and the first source of 51[Hz] (s2) was -0.64, while one for second source of 51[Hz] (s3) was -0.59.

Although the source of s3 simulated to have no correlation with the source of s1, this result indicated high correlation. This false correlation was considered to be caused by effect of wide skirts of estimated sources of s2 result from lower spatial resolution of original sLORETA.

## IV. DISCUSSION

By using simulated data, we demonstrated that our proposed method could estimate correlated sources even under the situation that non-correlated sources have same frequency as correlated sources.

For source estimation with EEG or MEG signals, a spatial filtering technique is recently applied as an alternative method for equivalent current dipole estimation technique. Non-adaptive type of spatial filtering technique, such as sLORETA, is reported to discriminate correlated sources. However, it may lead to inaccurate results due to its low spatial resolution. Therefore, in the present study, we proactively utilized the identified information in sensor level analysis (e.g. cross-correlation map and correlation topography), which allow us to focus on target sources. Our proposed approach can provide many advantages for analysis of connectivity and source estimation: 1) Confirmation of correlation in sensor level analysis make sure existence of significant characteristics. 2) By using spatial filtering technique in frequency domain, higher signal to noise analysis can be achieved because source estimation at identified frequency will exclude non-target activities in other frequency bands. 3) Correlated source can be focused by sensor signal weighting with correlation topography and modulated spectrum magnitude by correlated sensor signal identified in sensor level analysis.

Our proposed method can be considered to incorporate results of sensor level analysis into solution of inverse problem. In turn, the method uses objective-based constraints to solve inverse problem. Therefore, to investigate other types of brain activities such as those with transient movement, results of appropriate sensor level analysis (e.g. time-frequency analysis with trigger of the movement initiation) should be incorporate as other types of objective-based constraints to solve the inverse problem.

We believe that the method we propose become helpful tool to reveal connections of neuronal activities.

## REFERENCES

- [1] Osipova D., Hermes D., Jensen O.. Gamma Power Is Phase-Locked to Posterior Alpha Activity. PLOS ONE, 2008, Vol 3, Issue 12: 1-7
- [2] Lange F.P., Jensen O., Bauerl M., Toni I. Interactions between posterior gamma and frontal alpha/beta oscillations during imagined actions. *frontiers in human neuroscience*, 2008 Vol.2 Article 7; 1-12
- [3] Sekihara, K., Sahani, M., Nagarajan, S.S. Localization bias and spatial resolution of adaptive and non-adaptive spatial filters for MEG source reconstruction. *Neuroimage* 2005, Vol.25: 1056–1067.
- [4] Sekihara K., Nagarajan S.S, Poeppel D., Marantz A., Miyashita Y. Reconstructing Spatio-Temporal Activities of Neural Sources Using an MEG Vector Beamformer Technique. *IEEE Trans. Biomed. Eng.* 2001, Vol.48:760– 771.
- [5] Pascual-Marqui R.D., Standardized low-resolution brain electromagnetic tomography (sLORETA): technical details. *Methods Find Exp. Clin. Pharmacol.* 2002, Vol.24 (Suppl. D), 5–12.
- [6] Terakawa, Y., Tsuyuguchi, N., Tanaka, H., Shigihara, Y., Sakamoto, S., Takami, T., Ohata, K., Quantitative analysis of MEG using modified sLORETA for clinical application. *Clin. Neurophysiol.* 2008, Vol.119: 1917–1922.
- [7] Sakamoto S., Tanaka H., Tsuyuguchi N., Terakawa Y., Ohata K., Inoue Y., Miki Y., Hara M., Takahashi Y., Nitta K., Sawa H., Satone A., Ide W., Hashimoto I., Kamada H. Quantitative imaging of spontaneous neuromagnetic activity for assessing cerebral ischemia using sLORETA-qm. *NeuroImage* 2010, Vol.49: 488–497
- [8] Zhi Zhang. A fast method to compute surface potentials generated by dipoles within multilayer anisotropic spheres. *Phys. Med. Biol.* 1995, Vol.40: 335-349